DNA Research, 2020, 0(0), 1–10
doi: 10.1093/dnares/dsaa007
Full Paper

Full Paper

Transcriptomic analysis of sea star development through metamorphosis to the highly derived pentameral body plan with a focus on neural transcription factors

Maria Byrne[1,2]*, Demian Koop[1], Dario Strbenac[3], Paula Cisternas[1], Regina Balogh[1], Jean Yee Hwa Yang[3], Phillip L. Davidson[4], and Gregory Wray[4,5]

[1]School of Medical Sciences, The University of Sydney, Sydney, NSW 2006, Australia, [2]School of Life and Environmental Sciences, The University of Sydney, Sydney, NSW 2006, Australia, [3]School of Mathematics and Statistics, The University of Sydney, Sydney, NSW 2006, Australia, [4]Department of Biology, Duke University, Durham, NC 27708, USA and [5]Center for Genomic and Computational Biology, Duke University, Durham, NC 27708, USA

* To whom correspondence should be addressed. Tel. +61 2 9351 5167. Fax. +61 2 9351 2813.
Email: maria.byrne@sydney.edu.au

Received 11 November 2019; Editorial decision 17 April 2020; Accepted 20 April 2020

Abstract

The Echinodermata is characterized by a secondarily evolved pentameral body plan. While the evolutionary origin of this body plan has been the subject of debate, the molecular mechanisms underlying its development are poorly understood. We assembled a *de novo* developmental transcriptome from the embryo through metamorphosis in the sea star *Parvulastra exigua*. We use the asteroid model as it represents the basal-type echinoderm body architecture. Global variation in gene expression distinguished the gastrula profile and showed that metamorphic and juvenile stages were more similar to each other than to the pre-metamorphic stages, pointing to the marked changes that occur during metamorphosis. Differential expression and gene ontology (GO) analyses revealed dynamic changes in gene expression throughout development and the transition to pentamery. Many GO terms enriched during late metamorphosis were related to neurogenesis and signalling. Neural transcription factor genes exhibited clusters with distinct expression patterns. A suite of these genes was up-regulated during metamorphosis (e.g. *Pax6*, *Eya*, *Hey*, *NeuroD*, *FoxD*, *Mbx*, and *Otp*). *In situ* hybridization showed expression of neural genes in the CNS and sensory structures. Our results provide a foundation to understand the metamorphic transition in echinoderms and the genes involved in development and evolution of pentamery.

Key words: developmental transcriptome, radial body plan, metamorphosis, starfish, *Parvulastra exigua*

1. Introduction

The unusual adult pentameral body plan of echinoderms and how it relates to the bilateral plan of other members of the superphylum Deuterostomia has long been the subject of debate among evolutionary biologists.[1–6] This morphology is derived as Cambrian fossils shows that the earliest echinoderms were bilateral as adults.[7,8]

Although the molecular and cellular mechanisms underlying embryo and larval development in echinoderms are well studied, especially for the sea urchin model,[5] the molecular basis of metamorphosis and adult body plan development is poorly understood because of the challenge to rear feeding larvae to the juvenile in most species.[9,10] Use of direct developing species that metamorphose soon after gastrulation together with application of sequencing technologies, is proving a powerful approach to address questions regarding the development and evolution of pentamery. The developmental transcriptomes of the sea urchins *Heliocidaris erythrogramma* and *H. tuberculata* have revealed differences in the embryonic gene regulatory networks of these direct and indirect developers, respectively, and the molecular changes involved with metamorphosis and development of pentamery.[11–15]

After decades of conjecture, the class relationships within the Echinodermata are now supported to comprise the Asterozoa (Asteroidea, Ophiuroidea), the Echinozoa (Echinoidea, Holothuroidea), and the basal Crinozoa (Fig. 1).[16] Although echinoids are a major model system for developmental biology, they have many derived traits with respect to the rest of Echinodermata. Early development in most echinoids is characterized by unequal cleavage with tiers of differently sized blastomeres, while in the other echinoderm classes, cleavage is equal. Sea urchins also have two mesodermal lineages, including skeletogenic and pigment cells that are not present in asteroid larval development. They also have the unique echinopluteus larva and the most radical echinoderm metamorphosis forming the juvenile almost entirely of axial elements (skeleton associated with water vascular system elements) with cohesion between the rays.[17] An unusual feature of the Echinoidea is the transversion and inversion of their HOX and ParaHOX clusters[18,19] with the former suggested to be related to the evolution of the unique sea urchin skeletal test and body form.[6] Asteroids, in comparison, have the ancestral-type echinoderm body with distinct and separate rays as well as having the bipinnaria, the ancestral dipleurula-type larva shared with hemichordates (Fig. 1). In addition, the asteroid HOX and ParaHOX clusters are intact and similar to that of other deuterostomes.[20,21] Thus, although the Echinoidea is an impressive group for evolution and development (evo-devo) research,[14,22] they are less suitable than the Asteroidea to generate insights into the origins and evolution of pentamery in the Echinodermata.[6]

Research on the molecular and cellular biology of asteroid development has focused on the embryos and larvae of the asterinid sea star *Patiria miniata*, a species with indirect development and for which extensive genomic resources are available.[23,24] To generate insights into the molecular processes underlying adult asteroid development and its radial body plan, we assembled *de novo* a reference developmental transcriptome for the closely related asterinid, *Parvulastra exigua*. This direct developing species forms the juvenile soon after gastrulation providing the opportunity to generate thousands of metamorphosing juveniles within 8–10 days.[25] *Parvulastra exigua* has benthic development with hatching delayed until the advanced brachiolaria stage when these larvae have a well-developed attachment complex (brachia and adhesive disc) to ensure that they remain attached to the substratum.[25,26] As for *H. erythrogramma*, [27–29] the evolution of lecithotrophic development in *P. exigua* has been the focus of studies of alternative larval life history modes in the Echinodermata.[25,30–33]

We used RNA-seq to determine transcription profiles across development in *P. exigua* incorporating six developmental stages from gastrula [1-day post-fertilization (dpf)] to the definitive juvenile (21 dpf). The transcriptome was used to explore changes in gene expression during metamorphosis and adult body plan development. Differential expression analysis was used to compare gene expression in the gastrula and larvae and between larva and late metamorphic development of the pentameral adult. Gene ontology (GO) analysis showed that many of the terms enriched in the late metamorphosis stage were related to neural development and signalling. Considering the close relationship between body plan anatomy and central nervous system (CNS) organization,[34,35] we investigated the expression profiles of known neurogenesis transcription factors[36] over the time course of development. We were interested to determine if there is a suite of adult development-specific neural genes because the adult CNS of *P. exigua*, as generally the case for sea stars, develops *de novo* at metamorphosis.[37–39] We also explored the spatial expression of some of these genes in the developing CNS and sensory structures. Our developmental RNA-seq analyses captured the changes in gene expression during the metamorphic transition to the pentameral adult body plan and provided a framework to investigate the development and evolution of the unusual echinoderm radial body plan and its deuterostome affinities.

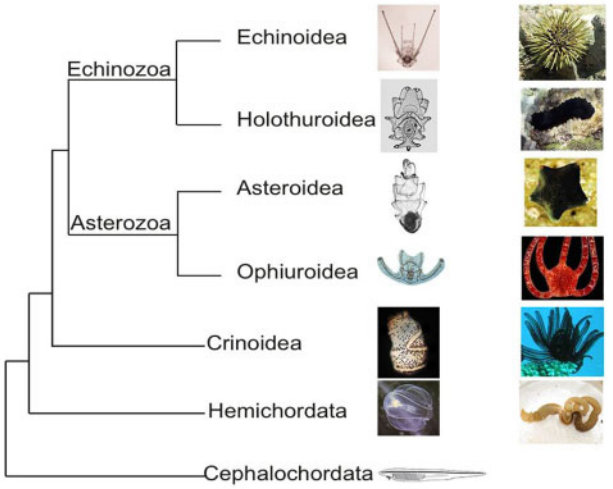

Figure 1. Echinoderm phylogeny showing class relationships, the Asterozoa (Asteroidea, Ophiuroidea), Echinozoa (Echinoidea, Holothuroidea), and basal Crinozoa and indicative relationship with the Hemichordata and Cephalochordata. Illustrations show adults and larvae. The Holothuroidea, Asteroidea, and Hemichordata have the ancestral-type feeding dipleurula larvae while the Echinoidea and Ophiuroidea have independently evolved the feeding pluteus larval form. The Crinoidea lack a feeding larva. Images provided: crinoid adult, A. Hoggett; crinoid larva H. Nakano; hemichordate images, B. Swalla, cephalochordate, P. Martinez.

2. Materials and methods

2.1. Sample collection, RNA preparation, sequencing and microscopy

Parvulastra exigua were collected near Sydney, Australia. The eggs were obtained by placing dissected ovaries in 10^{-5} M 1-Methyladenine (Sigma) in filtered sea water (FSW 1.0 µm Millipore) and fertilized using sperm removed from the testes. Three biological replicate cultures were established each using the gametes from multiple parents in completely unique crosses. The embryos and larvae were reared at 20°C as described by Byrne.[25] We sampled six developmental stages from each replicate: gastrula (1 dpf), early brachiolaria (3 dpf), hatched brachiolaria with the 5-lobed hydrocele

(6 dpf), flexed brachiolaria with the juvenile rudiment region (early metamorphosis) (10 dpf), metamorphic juvenile (12 dpf), and the definitive juvenile (21 dpf) (Fig. 2A–I). The samples were placed in RNAlater (Sigma) and stored frozen at −20°C until use. RNA was extracted using the RNeasy kit (Qiagen). RNA quantity was measured using a NanoDrop and quality was assessed with a BioAnalyzer. Libraries were prepared by Duke Center for Genomic and Computational Biology from 4 µg total RNA per sample using the Illumina Tru-Seq Library Preparation Kit and sequenced on an Illumina Hi-Seq 2000 with 50 bp paired end reads.

2.2. Microscopy

For confocal microscopy, specimens were fixed in 2.5% glutaraldehyde (ProSciTech, Australia) in filtered seawater (FSW 1.0 µm Millipore) for 1–2 h, washed in FSW, dehydrated in an ethanol series to 70% (v/v) ethanol in Milli-Q water and stored at 4°C. They were then dehydrated to 100% ethanol and cleared in 2:1 (v/v) benzyl benzoate/benzyl alcohol and mounted in a coverslip-sealed chamber. The specimens, autofluorescent from the glutaraldehyde fixation, were viewed in an Olympus FluoView 1000 laser scanning system (v.1.7.1.0) linked to an Olympus IX81 inverted microscope. They were excited at λ_{ex} 633 nm with a helium–neon laser and detected at λ_{em} 645–745 nm. Developing stages were also photographed using a DF13 Olympus camera mounted on an Olympus BX60 microscope.

2.3. Transcriptome assembly and annotation

Paired-end RNA-seq reads were generated on six stages of development in three biological replicates. Adapters and low-quality bases with quality value less than 20 were removed with cutadapt version 1.13.[40] Any resulting reads shorter than 40 bases were eliminated from further analysis. Assembly of short reads into putative transcripts was performed with Trinity version 2.4.0.[41] Default settings were used to produce the reference transcriptome (N50 = 3,676 bp, range of transcript lengths is 201–36,276 bp). To quantitate the assembled transcripts, RSEM version 1.3.0[42] was used with the paired-end setting and Bowtie2[43] was used by RSEM to map the reads to the transcriptome. Transcriptome sequences were annotated using BLASTn v. 2.6.0[44] to the recently released *P. miniata* genome version 2.0 gene models (www.echinobase.org/Echinobase/PmAbout, May 2017, date last accessed). A transcript was associated with a gene if the match had an e-value $<1 \times 10^{-20}$. The annotated set of transcripts is represented by significant hits to 23,502 unique *P. miniata* gene models, which include 7,575 distinct gene descriptions of transcripts within the assembly. A tool to visualize gene expression profiles from gastrula to definitive juvenile was developed and is available at http://shiny.maths.usyd.edu.au/starfishTimecourse/.

2.4. Variation in gene expression across the six developmental stages

For time course analyses, transcript abundance estimates were transformed as log2 (FPKM + 1) to remove the relationship between mean and variance. Gene-level analyses were done by choosing the most variable transcript associated with a particular gene. Principal components analysis of these data was carried out using the *prcomp* function in R version 3.4.2. The reduced dimension representation of gene abundances was plotted using 'autoplot' from the CRAN package *ggfortify*.[45]

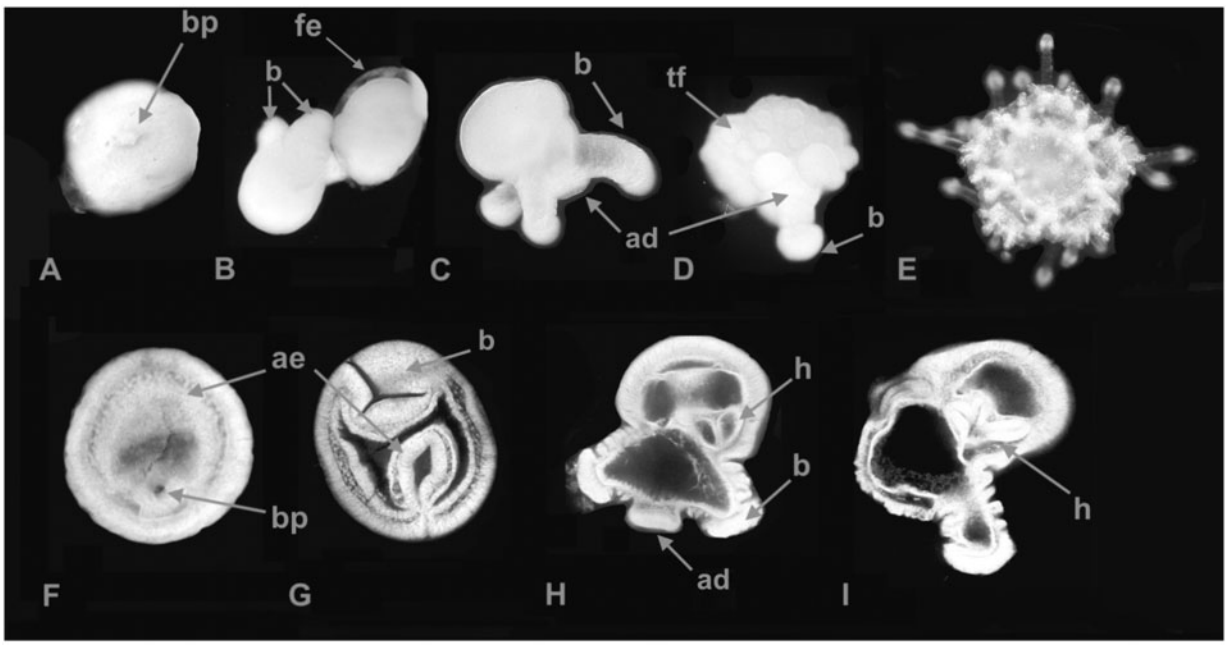

Figure 2. *Parvulastra exigua* (live images: A–E; confocal microscope sections: (F–I) including stages used for the developmental transcriptome. (A) Gastrula, one-day post fertilization (dpf) from the vegetal pole perspective to show the blastopore (bp) which subsequently closes. (B) Two early brachiolaria larvae (3 dpf). The left larva has hatched and the one on the right is emerging from the fertilization envelope (fe). b, brachia (C) Tripod brachiolaria (6 dpf) with well-developed brachia and adhesive disc (ad) that are used for attachment to the substratum. (D) Late metamorphosis (12 dpf) the attachment complex is being resorbed as the tube feet (tf) take over the role of benthic attachment. (E) Juvenile (20 dpf). (F) Section through the middle of a gastrula (1dpf) with the vegetal pole indicated by the blastopore at the bottom of the image and opening into the archenteron (ae). (G) Section through an unhatched early brachiolaria (3 dpf) with right and left coeloms evident on either side of the archenteron. (H and I) Mid-sections through tripod brachiolaria larvae at 6dpf (H) and 10 dpf (I) showing the developing hydrocoel (h) during metamorphosis (A, B, and D–H from 8, with permission). Scale bars = 100 μm.

2.5. Differential expression and GO analysis

Pairwise differential expression analyses were carried out between gastrula and hatched brachiolaria as well as hatched brachiolaria and late metamorphosis stages. To compare changes in abundance of each gene between timepoints, the read counts of every contig belonging to a particular gene were summed to the gene-level according to the best significant BLAST hit to *P. miniata* gene models (www.echinobase.org/Echinobase/PmAbout). At least five read counts in two or more samples per gene was required to be included in the pairwise differential expression analyses. After filtering, 13,358 and 13,333 distinct genes (from the total set of 23,502) remained for the gastrula vs. hatched brachiolaria comparison and the stages and the hatched brachiolaria vs. late metamorphosis comparison, respectively. The edgeR package v3.18.1[46] was used to perform the differential expression analyses. First, read counts were normalized using the *calcNormFactors* function in edgeR and *estimateDisp* function was used to estimate dispersion. Differential expression estimates were computed using the package's *exactTest* function for each pairwise comparison. Genes with an absolute log2 fold-change ≥ 2 and false-discovery rate $\leq 5\%$ were considered significantly differentially abundant between developmental stages (Supplementary data 1). Volcano plots were generated with *ggplot2*.[47]

GO analysis was undertaken to determine which 'Biological Processes' were enriched among the up-regulated genes during metamorphosis and juvenile development. GO annotations were retrieved according to significant contig hits (e-value $\leq$ 1e−20)[48] and compiled with Blast2GO[49] (Supplementary data 2). The 'piano' R package v1.16.4[50] was used to test for enrichment of GO terms relating to 'Biological Processes' in sets of significantly differentially abundant genes between developmental stages on a background set of all *P. miniata* genes included in the differential expression analysis. REVIGO[51] was used to summarize and visualize enriched GO terms from these analyses.

2.6. Neural genes

As the GO analysis showed that many of the terms enriched in late metamorphosis were related to neural development we searched the transcriptome for genes that encode transcription factors known to be involved in neurogenesis in echinoderms and other deuterostomes.[11,36,52] We analysed the expression profiles of 40 of these genes following a similar analysis of expression through metamorphosis in *H. erythrogramma*.[11] Expression profiles were analysed using the online Shiny application (See Supplementary Fig. 1). We were particularly interested in identifying examples of increase or decrease and peaks of expression during the pre-metamorphic, metamorphic, and post-metamorphic stages. Expression profiles were plotted with R 3.0.3,[53] where coloured dots represent the expression values of the three biological replicates (Supplementary Fig. 1).

2.7. Whole mount *in situ* hybridization

Spatial expression of *Pax6*, *Eya*, *SoxB*, and *Otx* was investigated using whole mount *in situ* hybridization (WMISH). Specimens were fixed in 4% paraformaldehyde in DEPC-treated FSW, dehydrated through a graded methanol series and stored in 100% methanol at −20°C. cDNA was synthesized using the Superscript III Reverse Transcriptase (Invitrogen) and gene-specific primers that were designed based upon sequences obtained from the *P. exigua* transcriptome. Amplified fragments were cloned into pGEM-T vector (Promega) and sequenced to confirmed gene identity. Probes for WMISH were synthesized as described by Byrne et al.[38] WMISH followed the methods of Byrne et al.[38] with the following amendments. Samples were pre-treated for 30 min in 6% hydrogen peroxide in 100% methanol prior to rehydration. Prior to hybridization, samples were incubated for 5 min in 0.1 M triethanolamine/5 µl/ml acetic anhydride. Probe detection was carried out using NBT/BCIP (Roche) in a detection buffer containing 10% polyvinyl alcohol. Reactions were stopped with several rinses in sterile water. Specimens were then dehydrated in a graded ethanol series, cleared in 1:2 benzyl benzoate/benzoic acid (v/v) and photographed (as above).

3. Results

3.1. Development of *Parvulastra exigua*

The developmental transcriptome time course included six developmental stages of *P. exigua*: gastrula (1 dpf), early brachiolaria (3 dpf), hatched brachiolaria (6 dpf), early metamorphic brachiolaria (10 dpf), metamorphosing juvenile (12 dpf), and the definitive juvenile (21 dpf) (Fig. 2A–I). This species lays its large eggs on the substratum in adhesive egg masses. The gastrulae and larvae remain within the fertilization envelope until the early brachiolaria larval stage and during this time the left and right coeloms develop (Fig. 2A, B, F, and G). Hatching is delayed until the larval attachment complex allows them to adhere to the substratum (Fig. 2B andC). The larvae have the tripod morphology of benthic sea star larvae with three larval arms equal in length and a hypertrophied attachment disk in the centre (Fig. 2B, C, H, and I). By Day 6, the core of the pentameral body plan, the 5-lobed hydrocoel develops (Fig. 2H andI). During subsequent days the juvenile rudiment develops and becomes evident on external view (Fig. 2D). By 10 dpf the larvae have the oral side of the developing juvenile directed towards the substratum and the adult tube feet are evident externally (Fig. 2D). The larval body is resorbed slowly as metamorphosis proceeds and the juvenile tube feet take over the role of attachment (Fig. 2D). By 21 dpf the definitive juvenile is well established (Fig. 2E).

3.2. Variation in gene expression across developmental stages

The PCA of developmental gene expression across the six stages showed that most of the variation was between the pre-metamorphic stages of development (PC1—62%), whereas only 18% of variation is explained by differences in the metamorphic and post-metamorphic stages (PC2—18%). Thus, PC1 and 2 captured 80% of the total variation within the gene expression dataset. The similarity between the early and late metamorphic and juvenile stages may be due to the prolonged metamorphosis of *P. exigua*. Variation across the developmental transcriptome distinguished the gastrula expression profile from all other stages (Fig. 3), likely indicative of major morphogenetic processes occurring at this stage of development.

3.3. Differential expression

To identify which genes had significant changes in expression through *P. exigua* development, pairwise differential expression analyses were carried out between three stages. We found 2,242 genes with significant differences in expression between gastrula and hatched brachiolaria (Fig. 4A) and 424 genes differentially expressed between hatched brachiolaria and late metamorphosis (Fig. 4A,

Supplementary data 1). In terms of both number of genes and magnitude of expression changes, there was far greater differential expression between gastrula and hatched brachiolaria than the later comparison. This result is consistent with the PCA (Fig. 3) in which PC1 clearly separates gastrula from subsequent developmental stages and reflects the key morphogenetic processes that occur during this stage of development. Indeed, among the most enriched GO terms of genes up-regulated at the gastrula stage are 'RNA splicing' ($P < 4.59e{-}6$) and 'cell differentiation' ($P < 5.75e{-}4$),

The genes that were significantly differentially abundant between early larvae (hatched brachiolaria) and the late metamorphosis stages included 113 genes that were more abundant at the hatched brachiolaria and 311 genes that were more abundant at late metamorphosis (Fig. 4, Supplementary data 1). Among the most enriched GO biological processes of genes significantly more abundant at late metamorphosis are terms relating to neural development and signalling (Fig. 5, Supplementary data 2). Other GO categories were related to transcription, cell signalling, and ion transport. Expression relating to these biological processes is consistent with development of the CNS and juvenile sensory structures between these two stages of development.

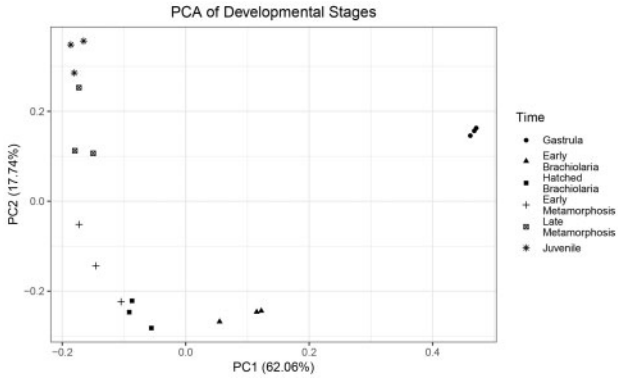

Figure 3. Principal component analysis of developmental gene expression across six stages of development in *P. exigua*. Most variation was between the pre-metamorphic stages (PC1–62%). Only 18% of variation is explained by differences in the metamorphic and post-metamorphic stages (PC2–18%). The PCA distinguishes the gastrula expression profile from all later developmental stages.

3.4. Temporal expression of neurogenesis transcription factors over development

The temporal expression profiles across the six developmental time points for 40 genes known to be involved in neurogenesis are shown in Supplementary Fig. 1. Specific genes involved in neurogenesis including *BarH1*, *Mbx*, *Gsx*, *Otp*, *FoxB*, *FoxD*, *Pax6*, *Hey*, *NeuroD*, *Ngn*, and *Hnf6* (see 36,52) are among the 311 genes more abundant during late metamorphosis. Although expression varied with respect to patterns of up-regulation or down-regulation over the time course of development, a few distinct profiles were evident (Fig. 6, Supplementary Fig. 1).

A group of important genes (e.g. *Otx*, *Six3/6*, *Rx*, *Emx*, *FoxM*, and *Dlx*) exhibited early up-regulation in the gastrula stage followed by a pre-metamorphic decrease after gastrulation through the larval and metamorphic stages (Fig. 6A). In some of these genes the decrease was not so marked (e.g. *Six3/6*) and others (e.g. *Otx* and *Dlx*) showed some increase in late metamorphosis and the juvenile stages (Fig. 6A).

A second striking pattern was seen in up-regulation of expression between gastrulation and the early larva followed by a decline and then by increased expression through metamorphosis and juvenile stages (Fig. 6B). This was seen for *Pax6*, *Otp*, *FoxD*, *Eya*, and *Hey*, among others (Fig. 6B, Supplementary Fig. 1).

In a third pattern, low expression in pre-metamorphic stages (gastrula to hatched brachiolaria) was followed by an up-regulation during metamorphosis (Days 10 and 12) (Fig. 6C). This included *FoxB*, *BarH1*, and *Mbx* (Fig. 6C), A number of genes that showed various expression profiles during pre-metamorphic development had peak

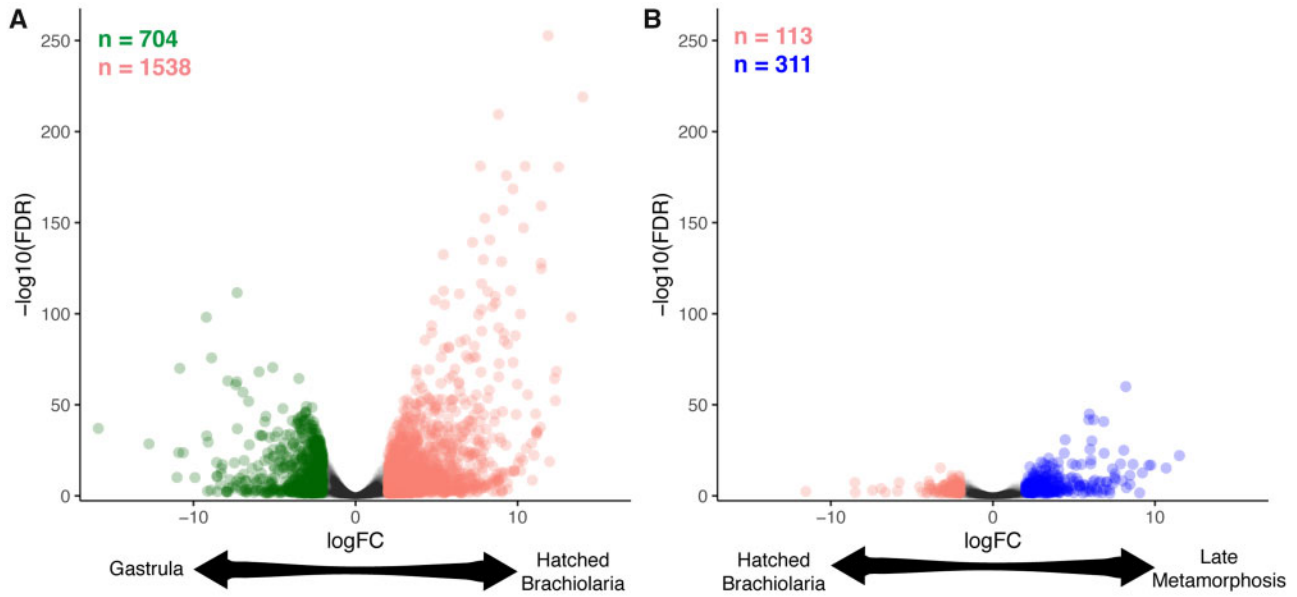

Figure 4. Volcano plot of expression changes between (A) gastrula and hatched brachiolaria larva and (B) hatched brachiolaria and late metamorphosis stages. Genes with a log2 fold-change (FC) greater than or equal to 2 and supported by a false-discovery rate (FDR) less than 5% are coloured according to the stage at which they are significantly up-regulated: gastrula (green), hatched brachiolaria (pink), and late metamorphosis (blue).

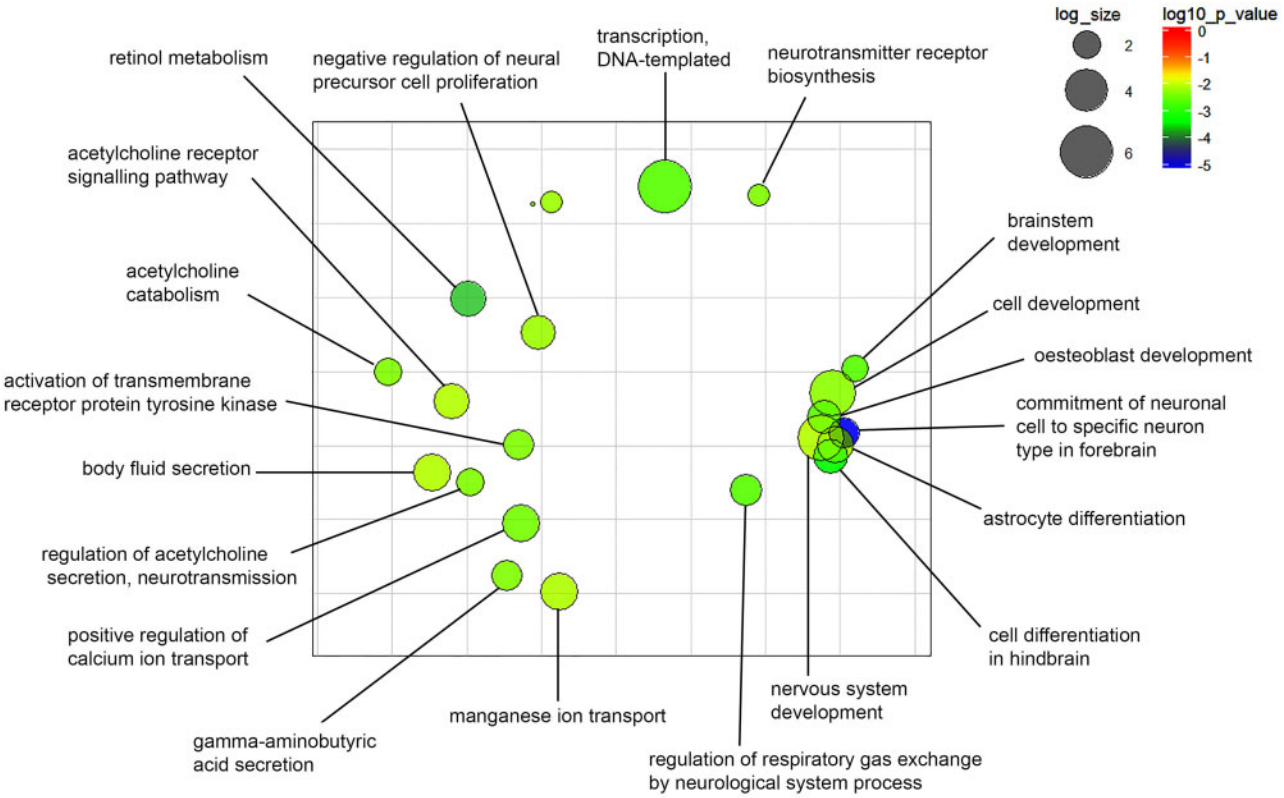

Figure 5. Multidimensional scaling plot of semantic similarity matrix generated from the top 30 enriched GO 'Biological Process' terms from genes significantly up-regulated during late metamorphosis relative to the hatched brachiolaria (larval) stage. GO term cluster representatives plotted as summarized by REVIGO. Bubble size reflects the frequency of the GO term in the Uniprot Gene Association Database and colour represents the log10 *P*-value of the GO term from the enrichment analyses. Genes up-regulated in the late metamorphosis stage are enriched for GO terms relating to neural development and signalling.

expression in the late metamorphosis and/or the juvenile stages, including *Nurr1*, *Isl*, *Hnf6*, *Meis*, *Pou4f2*, *ebf3*, *Gad*, and *Brn1/2/4* (Supplementary Fig. 1).

Finally, some genes were transiently up-regulated in the early larval stage e.g. *Ngn*, *Hey*, *Otp*, and *FoxD* (Supplementary Fig. 1). *Nkx2.1* had the highest expression at the gastrula and early brachiolaria stages with down-regulation thereafter (Supplementary Fig. 1).

3.5. Spatial expression of neurogenesis genes in the metamorphic juvenile

The asteroid CNS is located on the surface ectoderm (i.e. not covered in skeleton as in other echinoderms) and so spatial gene expression in the radial nerve cord and associated sensory structures (eye spot, tube feet) are evident on surface view. *In situ* hybridization indicated that the expression domain of *Otx* became focussed to the CNS (Fig. 7A). *Otx* has high temporal expression in early embryos (Fig. 6A) and its lower expression in later development indicates down-regulation. However, *Otx* is strongly expressed in the developing CNS (Fig. 7A). *Eya* is up-regulated during metamorphosis (Fig. 6B) and its expression domain is also associated with the CNS (Fig. 7B). The temporal expression of *Pax6* increases during metamorphosis and in the juvenile (Fig. 6B). This gene is strongly expressed in the eye spot at the end of the radial nerve cord and in the pairs of tube feet (Fig. 7D). *SoxB1* is also expressed in the tube feet and eye spot (Fig. 7C). This gene has a uniform high expression through development (Supplementary Fig. 1).

4. Discussion

The bilateral larva to pentameral juvenile metamorphic transition heralds a distinct phase in gene expression in *P. exigua*, as also the case for the sea urchin *H. erythrogramma*,[11] and other marine invertebrates that undergo a larva to juvenile metamorphic transition.[54]. This highlights the distinct larval and adult developmental modules and their likely association with distinct gene regulation. The transcriptomic resources developed here for *P. exigua*, and previously for *H. erythrogramma*,[11,14] with extensive coverage of the metamorphic stages, provide the basis to investigate changes in gene expression during development of pentamery and to explore deuterostome affinities of the unique echinoderm body plan.

The PCA showed that gene expression in the gastrula stage of *P. exigua* was separate from that in the other stages, as also found for *H. erythrogramma*.[11]). This was also reflected in the differential gene expression analysis and may be explained in the regulation of tissue specification and unique morphogenetic processes that occur during gastrulation.[55] The PCA also showed that gene expression was less variable across the metamorphic and juvenile stages compared with the pre-metamorphic stages. In contrast, the change in gene expression associated with metamorphosis in *H. erythrogramma* is more temporally marked.[11] This difference may be due to the benthic mode development in *P. exigua* where metamorphosis is slow (over 5–7days).[25] The larvae remain attached as their body degenerates in parallel with development of the adult podia. In *H. erythrogramma*, the metamorphic transition following settlement of the planktonic larva is much shorter.[11] For *P. exigua*, it

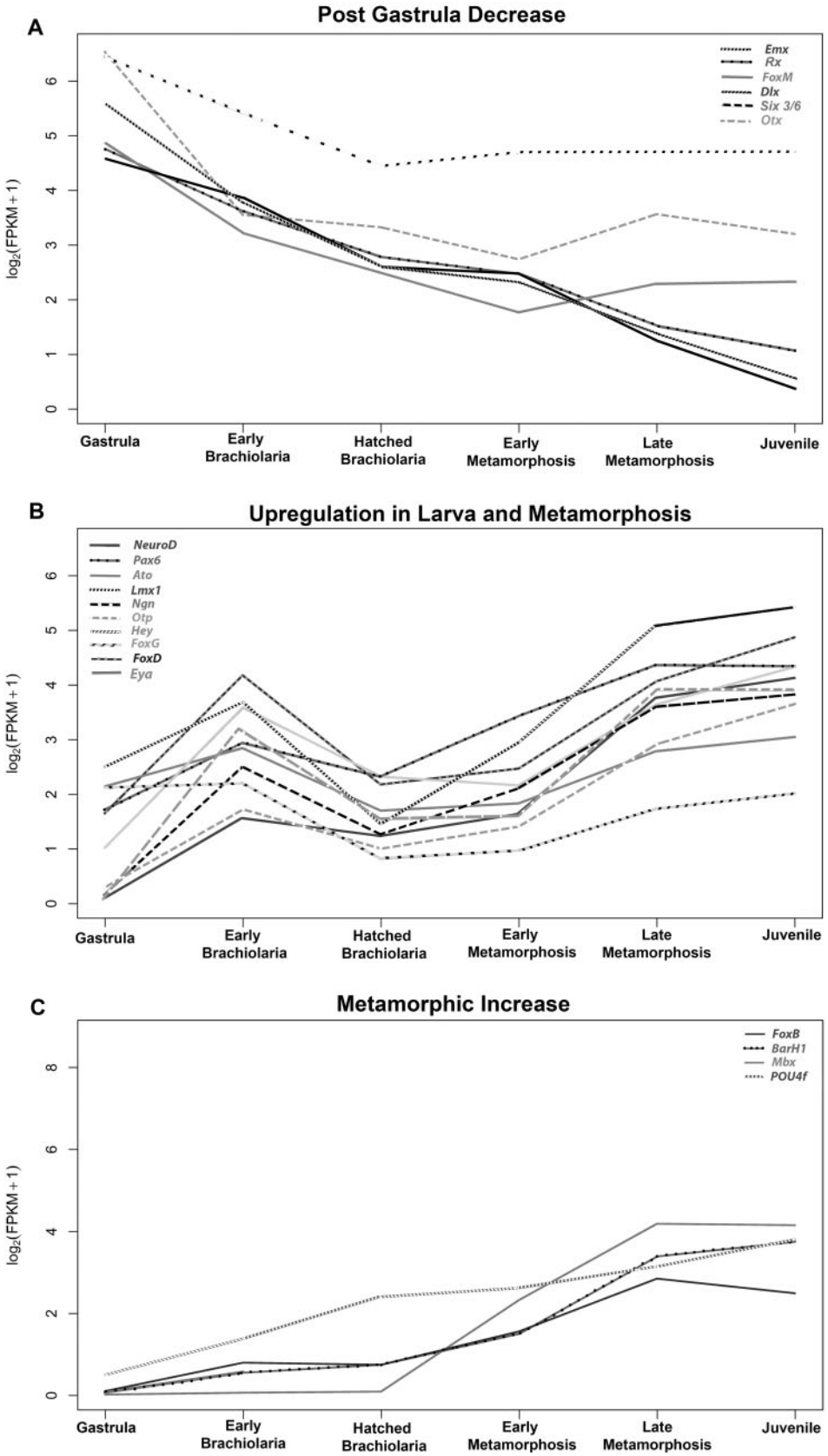

Figure 6. Temporal expression profiles in *P. exigua* of putative neurogenic genes in three profiles, (A) Post-gastrula decrease, (B) up-regulation between gastrulation and the early larval stages followed by a decrease and an up-regulation at metamorphosis and juvenile stages, and (C) low expression in pre-metamorphic stages followed by an up-regulation during metamorphosis. The Fragments per kilobase of transcript per million mapped read (FPKM), log transformed, were plotted for the six developmental stages (see Supplementary Fig. 1).

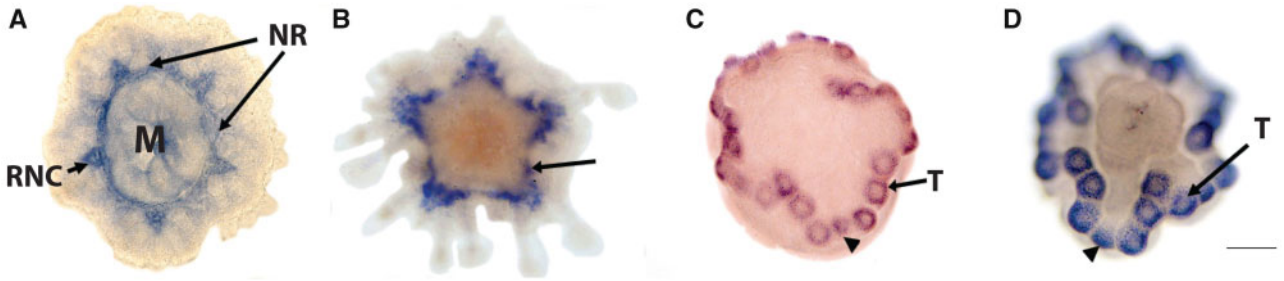

Figure 7. *In situ* hybridization of spatial expression of neurogenic genes in the developing juvenile *P. exigua*. (A) *Otx* expression in the oral nerve ring (NR) and the radial nerve cord (RNC). (B) *Eya* expression associated with the nervous system (arrow). (C) *SoxB1* and (D) *Pax6* expression in the developing juvenile tube feet (T) and eyespot (arrowhead). The specimen in C is an early metamorphosing juvenile and so lacks the mouth opening. M, mouth. Scale bars = 50 μm.

was surprising, that gene expression in the older definitive juvenile (21days old) was not more distinct compared with the metamorphic stages (10 and 12days old).

We investigated the larva–juvenile transition in GO analysis of differential gene expression between pre-(hatched brachiolaria) and post-metamorphic (late metamorphosis) stages. Differential expression analysis demonstrates an especially pronounced up-regulation in expression of many genes at late metamorphosis relative to hatched brachiolaria in terms of both fold-change magnitude and number of genes (311) (Supplementary Data 1). This result reflects a large transcriptomic shift associated with the life history transition to a benthic juvenile. Many of the GO terms enriched in differentially expressed genes were related to neural development, as also found for *H. erythrogramma*.[11] Many of the genes known to be expressed during development of the sea urchin larval nervous system[36] were expressed in *P. exigua* (Supplementary Fig. 1). High expression of *Nkx2.1* in the gastrulae and early larvae of *P. exigua* is similar to the timing of expression of this gene in development of the feeding larvae in echinoids and asteroids where it is associated with patterning the larval nervous system.[56,57] For *P. exigua* expression of *Nkx2.1* in the gastrula and early brachiolaria may be associated with development of the larval nervous system,[58] although this system is reduced in the benthic larva of this species. In addition, high expression of *Rx* and *Six3/6* at the gastrula stage is consistent with the stage of expression of these genes in *P. miniata* where they are involved in establishment of neurogenic territories in the larva.[23] For *Otx*, up-regulation during gastrulation in *P. exigua* is likely to be due to its conserved function in endoderm development during this embryonic stage in sea stars.[59,60]

There does not appear to be a set of larva or adult specific neural genes in *P. exigua*, as also for *H. erythrogramma*.[11,15] The bimodal-like pattern of expression with initial up-regulation between gastrula and early larvae followed by a decrease and then up-regulation during metamorphosis and remaining high in the post-metamorphic juvenile was seen many of the neural transcription factor genes. This indicates roles for these genes in embryogenesis and juvenile development.

We expected that renewal of neurogenesis as the adult nervous system develops during metamorphosis[38] would be associated with up-regulation of neural transcription factors. Indeed, for *P. exigua*, a suite of neural genes was more richly expressed during metamorphosis and post-metamorphosis. The *P. exigua* and *H. erythrogramma* transcriptomes provide an opportunity for an asteroid–echinoid comparison with respect to genes that may be involved with CNS development as well as patterning the pentameral body, as these processes occur simultaneously. In *H. erythrogramma* genes that peak during rudiment development include *SoxC*, *Barh1*, *Hnf6*, *Sp8*, and *Meis* and those that peak after metamorphosis in the juvenile include *Mbx*, *Isl*, *Nurr1*, *Pou4f*, and *Otp*.[11] These genes exhibited a similar expression pattern in *P. exigua* but were more spread across the rudiment and juveniles stages, likely due to the gradual metamorphosis of this species. Thus, despite the ~500 million-yr-old asteroid–echinoid divergence from a common ancestor, there is strong conservation in expression of neural transcription factors in metamorphosis and juvenile development. This indicates the essential roles of these genes during these life history stages, a suggestion that needs to be addressed through functional studies. It will be of interest to compare the expression of neural transcription factors in the adult asteroid and echinoid from biological and functional perspectives and their differential expression with respect to body plan and neurogenesis.

As CNS morphogenesis parallels the development of pentamery, exploring potential links between these two will be informative. In *P. exigua*, *Hox4*, a gene deleted from the sea urchin HOX cluster, is expressed in the hydrocoel lobes in the larva and in the developing CNS post-metamorphosis, as is *Engrailed*.[38,61] We show here that *Otx* and *Eya*, and previously,[38] that *Eng* are also expressed in the developing CNS of this species. In *H. erythrogramma* *Six1/2* is expressed in the hydrocoel lobes and in the developing CNS and other putative neurogenic genes (e.g. *Eya*, *Tbx2/3*, and *Msx*) are also expressed in hydrocoel development.[15] *Pax6*, *Otx*, and *Six3/6* are expressed in the developing sea urchin CNS.[13,62–64] The spatial expression domain of *Otx* is focussed on the CNS during metamorphosis. This shows the importance of determining the spatial expression of transcription factor genes which otherwise appear to be down-regulated in transcriptome analysis, as noted for retinal determination genes in sea urchin development.[13]

In *P. exigua*, *Pax6* is strongly expressed in the eye spot at the tip of the radial nerve cord where it ends at the primary podium and in the tube feet, structures that are considered to be photosensory.[13,65] This is consistent with expression of *Pax6* in photosensory structures in diverse species.[66,67] In *H. erythrogramma* and other sea urchins *Pax6* is expressed in the primary podia and tube feet.[13,65]

While most research on echinoderm neurogenesis has focussed on the larval nervous system, with many fundamental advances and discoveries made,[23,52,68] this structure is not considered to be relevant to discussions on relationships with the chordate nervous system.[69] Although adult echinoderms are not cephalized, their CNS has many structural similarities with the chordate nerve cord.[70–72] For example, the oral nerve ring and radial nerve cord have a neuroepithelium containing nerve cell bodies and an axonal neuropil with glial cells, analogous to the grey and white matter of the vertebrate spinal cord,

respectively.[71,73] With respect to spatial expression of neural genes, the open ambulacral system of the Asteroidea with the CNS in the surface ectoderm is particularly amenable to compare cell and tissue level molecular biology of the echinoderm nervous system with that of the chordates.

As basal deuterostomes, echinoderms are in a phylogenetic position key to understanding evolutionary origins of the chordate nervous system. The timing of expression of many neural transcription factors coincided with CNS development indicating conserved roles in nerve cord patterning. However, their location of expression and function in adult echinoderm neurogenesis remain to be determined. It appears that a focus on the molecular mechanisms underlying development of the adult echinoderm CNS will be informative with respect to determining chordate affinities.

The echinoid–asteroid comparisons made here, based on temporal expression patterns in developmental transcriptome analysis are only indicative, but the genomic resources for *P. exigua* (this study) and *H. erythrogramma*[11,14] provide the tools to investigate the molecular mechanisms underlying development of the adult echinoderm and its unusual pentameral body plan in basal (Asteroidea) and more derived (Echinoidea) classes. In addition, the ability to readily generate 1000s of metamorphic and juvenile stages of these direct developing species presents a unique model system for detailed spatial studies of gene expression in the development of pentamery and the biological processes underlying echinoderm–deuterostome affinities and evolution.

Acknowledgements

Thanks to L. Elia and H. Campbell for assistance. Animals were collected under permit from New South Wales Department of Primary Industries.

Accession numbers

Data generated and transcriptome assembled for this study are available on the NCBI Sequence Read Archive via accession number PRJNA587360.

Funding

This work was supported by an Australian Research Council Discovery Grant (DP120102849) (MB, GW, JHWY) and the National Science Foundation Grant (IOS-1929934). All aspects of this study were conducted independently by the authors without funding body involvement.

Conflict of interest

None declared.

Supplementary data

Supplementary data are available at DNARES online.

References

1. Hyman, L.H. 1955, *The Invertebrates: Echinodermata IV*, McGraw-Hill: NY,. [Database]
2. Hotchkiss, F.H.C. 1998, A "rays-as-appendages" model for the origin of pentamerism in echinoderms, *Palaeobiology*, **24**, 200–14.
3. Smith, A.B. 2005, The pre-radial history of echinoderms, *Geol. J.*, **40**, 255–80.
4. Morris, V.B. 2012, Early development of coelomic structures in an echinoderm larva and a similarity with coelomic structures in a chordate embryo, *Dev. Genes. Evol.*, **222**, 13–323.
5. Arnone, M.I., Byrne, M. and Martinez, P. 2015, Echinodermata. In: Wanninger A, ed. *Evolutionary Developmental Biology of Invertebrates 6 Deuterostomia*, Springer: New York, pp. 1–58.
6. Byrne, M., Martinez, P. and Morris, V. 2016, Evolution of a pentameral body plan was not linked to translocation of anterior Hox genes: the echinoderm HOX cluster revisited, *Evol. Dev.*, **18**, 137–43.
7. Zamora, S. and Smith, A.B. 2012, Cambrian stalked echinoderms show unexpected plasticity of arm construction, *Proc. Biol. Sci.*, **279**, 293–8.
8. Smith, A.B., Zamora, S. and Álvaro, J.J. 2013, The oldest echinoderm faunas from Gondwana show that echinoderm body plan diversification was rapid, *Nat. Comm.*, **4**, 1385.
9. Wray, G.A., Kitazawa, C. and Miner, B. 2004, Culture of echinoderm larvae through metamorphosis, *Methods Cell Biol.*, **74**, 75–86.
10. Hodin, J., Heyland, A., Mercier, A., et al. 2019, Culturing echinoderm larvae through metamorphosis. In: Foltz KR, Hamdoun A, eds, *Methods in Cell Biology – 150*. Elsevier: New York, pp. 125–169.
11. Wygoda, J.A., Yang, Y., Byrne, M., et al. 2014, Transcriptomic analysis of the highly derived radial body plan of a sea urchin, *Genome Biol. Evol.*, **6**, 964–73.
12. Byrne, M., Koop, D., Cisternas, P., et al. 2015, Transcriptomic analysis of Nodal-and BMP-associated genes during juvenile development of the sea urchin Heliocidaris erythrogramma, *Mar. Genomics*, **24**, 41–5.
13. Byrne, M., Koop, D., Morris, V.B., et al. 2018, Expression of genes and proteins of Pax-Six-Eya-Dach network in the metamorphic sea urchin: insights into development of the enigmatic echinoderm body plan and sensory structures, *Dev. Dyn.*, **247**, 239–49.
14. Israel, J.W., Martik, M.L., Byrne, M., et al. 2016, Comparative developmental transcriptomics reveals rewiring of a highly conserved gene regulatory network during a major life history switch in the sea urchin genus Heliocidaris, *PLoS Biol.*, **14**, e1002391.
15. Koop, D., Cisternas, P., Morris, V.B., et al. 2017, Nodal and BMP activity during adult rudiment formation in Heliocidaris erythrogramma: insights into patterning the pentameral echinoderm body plan, *BMC Dev. Biol.*, **17**, 4.
16. Cannon, J.T., Kocot, K.M., Waits, D.S., et al. 2014, Phylogenetic resolution of the hemichordate and echinoderm clade, *Curr. Biol.*, **24**, 2827–32.
17. David, B. and Mooi, R. 1998, Major events in the evolution of echinoderms viewed by the light of embryology. In Mooi R, Telford M, eds, *Echinoderms: San Franscisco*, Balkema: Rotterdam, p 21–28.
18. Arnone, M.I., Rizzo, F., Annunciata, R., et al. 2006, Genetic organization and embryonic expression of the ParaHox genes in the sea urchin S. purpuratus: insights into the relationship between clustering and colinearity, *Dev. Biol.*, **300**, 63–73.
19. Cameron, R.A., Rowen, L., Nesbitt, R., et al. 2006, Unusual gene order and organisation of the sea urchin HOX cluster, *J. Exp. Zool. B. (Mol. Dev. Evol.)*, **306B**, 45–58.
20. Annunziata, R., Martinez, P. and Arnone, M.I. 2013, Intact cluster and chordate-like expression of ParaHox genes in a sea star, *BMC Biol.*, **11**, 68.
21. Baughman, K.W., McDougall, S., Cummins, S., et al. 2014, Genomic organization of Hox and ParaHOX clusters in the echinoderm, Acanthaster Planci, *Genesis*, **52**, 952–8.
22. Raff, R.A. and Byrne, M. 2006, The active evolutionary lives of echinoderm larvae, *Heredity*, **97**, 244–52.
23. Cheatle Jarvela, A.M., Yankura, K.A. and Hinman, V.F. 2016, A gene regulatory network for apical organ neurogenesis and its spatial control in sea star embryos, *Development*, **143**, 4214–23.
24. Cary, G.A. and Hinman, V.F. 2017, Echinoderm development and evolution in the post-genomic era, *Dev. Biol.*, **427**, 203–11.
25. Byrne, M. 1995, Changes in larval morphology in the evolution of benthic development by Patiriella exigua (Asteroidea), a comparison with the larvae of Patiriella species with planktonic development, *Biol. Bull.*, **188**, 293–305.

26. Morris, V.B., Selvakumaraswamy, P., Whan, R. and Byrne, M. 2009, Development of the five primary podia from the coeloms of a sea star larva: homology with the echinoid echinoderms and other deuterostomes, *Proc. R. Soc. B*, **276**, 1277–84.
27. Wray, G.A. and Raff, R.A. 1991, Rapid evolution of gastrulation mechanisms in a sea urchin with lecithotrophic larvae, *Evolution*, **45**, 1741–50.
28. Raff, R.A. 1992, Direct-developing sea-urchins and the evolutionary reorganization of early development, *Bioessays*, **14**, 211–8.
29. Wray, G.A. 1996, Parallel evolution of nonfeeding larvae in echinoids, *Syst. Biol.*, **45**, 308–22.
30. Byrne, M. 2007, Life history evolution in the Asterinidae, *Integr. Comp. Biol.*, **46**, 243–54.
31. Byrne, M. 2013, Asteroid evolutionary developmental biology and ecology. In: Lawrence J, ed. *The Ecology of the Asteroidea*, Hopkins Press: Baltimore, pp. 51–58.
32. Hart, M.W., Byrne, M. and Smith, M.J. 1997, Molecular phylogenetic analysis of life-history evolution in asterinid starfish, *Evolution*, **51**, 1848–59.
33. Morris, V.B., Selvakumaraswamy, P., Whan, R., et al. 2011, The coeloms in a late brachiolaria larva of the asterinid sea star Parvulastra exigua: deriving an asteroid coelomic model, *Acta. Zool.*, **92**, 266–75.
34. Nielsen, C. 1999, Origin and of the chordate nervous system – and the origin of the chordates, *Dev. Genes Evol.*, **209**, 198–205.
35. Holland, N.D. 2003, Early central nervous system evolution, *Nat. Rev. Neurosci.*, **4**, 617–27.
36. Burke, R.D., Angerer, L.M., Elphick, M.R., et al. 2006, A genomic view of the sea urchin nervous system, *Dev. Biol.*, **300**, 434–60.
37. Byrne, M., Cisternas, P. and Koop, D. 2001, Evolution of larval form in the sea star genus Patiriella: conservation and change in the larval nervous system, *Dev. Growth Differ.*, **43**, 459–68.
38. Byrne, M., Cisternas, P., Elia, L., et al. 2005, Engrailed is expressed in larval development and in the radial nervous system of Patiriella sea stars, *Dev. Genes Evol.*, **215**, 608–17.
39. Byrne, M. and Cisternas, P. 2002, Development and distribution of the peptidergic system in larval and adult Patiriella: comparison of the sea star bilateral and radial nervous systems, *J. Comp. Neurol.*, **451**, 101–14.
40. Martin, M. 2011, Cutadapt removes adapter sequences from high-throughput sequencing reads, *EMBnet J.* , **17**, 10–2.
41. Grabherr, M.G., Haas, B.J., Yassour, M., et al. 2011, Full-length transcriptome assembly from RNA-Seq data without a reference genome, *Nat. Biotechnol.*, **29**, 644–52.
42. Li, B. and Dewey, C.N. 2011, RSEM: accurate transcript quantification from RNA-Seq data with or without a reference genome, *BMC Bioinform.*, **12**, 323.
43. Langmead, B. and Salzberg, S. 2012, Fast gapped-read alignment with Bowtie 2, *Nat. Methods*, **9**, 357–9.
44. Camacho, C., Coulouris, G., Avagyan, V., et al. 2009, BLAST+: architecture and applications, *BMC Bioinform.*, **10**, 421.
45. Tang, Y., Horikoshi, M. and Li, W. 2016, ggfortify: unified interface to visualize statistical result of popular R packages, *R J.*, **8**, 474–89.
46. Robinson, M.D., McCarthy, D.J. and Smyth, G.K. 2010, edgeR: a Bioconductor package for differential expression analysis of digital gene expression data, *Bioinformatics*, **26**, 139–40.
47. Wickham, H. 2016, *ggplot2: Elegant Graphics for Data Analysis*, Springer-Verlag: NY.
48. UniProt, C. 2015, UniProt: a hub for protein information, *Nucleic Acids Res.*, **43**, D204–12.
49. Conesa, A., Gotz, S., Garcia-Gomez, J.M., et al. 2005, Blast2GO: a universal tool for annotation, visualization and analysis in functional genomics research, *Bioinformatics*, **21**, 3674–6.
50. Varemo, L., Nielsen, J. and Nookaew, I. 2013, Enriching the gene set analysis of genome-wide data by incorporating directionality of gene expression and combining statistical hypotheses and methods, *Nucleic Acids Res.*, **41**, 4378–91.
51. Supek, F., Bosnjak, M., Skunca, N., et al. 2011, REVIGO summarizes and visualizes long lists of gene ontology terms, *PLoS One*, **6**, e21800.
52. Hinman, V.F. and Burke, R.D. 2018, Embryonic neurogenesis in echinoderms, *Dev. Biol.*, **7**, e316.
53. Team, R.C. 2012, *R: A Language and Environment for Statistical Computing*, R Foundation for Statistical Computing: Vienna, Austria.
54. Zheng, Z., Hao, R., Xiong, X., et al. 2019, Developmental characteristics of pearl oyster Pinctada fucata martensii: insight into key molecular events related to shell formation, settlemente and metamorphosis, *BMC Genomics*, **20**, 122.
55. Martik, M. and McClay, D.R. 2017, New insights from a high-resolution look at gastrulation in the sea urchin, Lytechinus variegatus, *Mech. Dev.*, **148**, 3–10.
56. Angerer, L.M., Yaguchi, S., Angerer, R.C. and Burke, R.D. 2011, The evolution of nervous system patterning: insights from sea urchin development, *Development*, **138**, 3613–23.
57. Yankura, K.A., Martik, M.L., Jennings, C.K. and Hinman, V.F. 2010, Uncoupling of complex regulatory patterning during evolution of larval developmemnt in echinoderms, *BMC Biol.*, **8**, 143.
58. Elia, L., Selvakumaraswamy, P. and Byrne, M. 2009, Nervous system development in feeding and nonfeeding asteroid larvae and the early juvenile, *Biol. Bull.*, **216**, 322–34.
59. Hinman, V.F., Nguyen, A.T. and Davidson, E.H. 2003, Expression and function of a starfish Otx ortholog, AmOtx: a conserved role for Otx proteins in endoderm development that predates divergence of the eleutherozoa, *Mech. Dev.*, **120**, 1165–76.
60. Hinman, V.F. and Davidson, E.H. 2007, Evolutionary plasticity of developmental gene regulatory network architecture, *Proc. Nat. Acad. Sci. USA*, **104**, 19404–9.
61. Cisternas, P. and Byrne, M. 2009, Expression of Hox4 during development of the pentamerous juvenile sea star, Parvulastra exigua, *Dev. Genes Evol.*, **219**, 613–8.
62. Nielsen, M.G., Popodi, E.M., Minsuk, S., et al. 2003, Evolutionary convergence in Otx expression in the pentameral adult rudiment in direct-developing sea urchins, *Dev. Genes Evol.*, **213**, 73–82.
63. Morris, V.B. and Byrne, M. 2005, Involvement of two Hox genes and otx in echinoderm body-plan morphogenesis in the sea urchin Holopneustes purpurescens, *J. Exp. Zool. B. Mol. Dev. Evol.,* **304B**, 456–67.
64. Morris, V.B. and Byrne, M. 2014, Oral-aboral identity displayed in the expression of HpHox3 and HpHox11/13 in the adult rudiment of the sea urchin Holopneustes purpurescens, *Dev. Genes Evol.*, **224**, 1–11.
65. Ullrich-Lüter, E.M., Dupont, S., Arboleda, E., et al. 2011, Unique system of photoreceptors in sea urchin tube feet, *Proc. Natl. Acad. Sci.*, **108**, 8367–72.
66. Vopalensky, P. and Kozmik, Z. 2009, Eye evolution: common use and independent recruitment of genetic components, *Phil. Trans. R. Soc. B*, **364**, 2819–32.
67. Fortunato, S.A.V., Leininger, S. and Adamska, M. 2014, Evolution of the Pax-Six-Eya-Dach network: the calcisponge case study, *EvoDevo*, **5**, 23.
68. Byrne, M, Nakajima, Y, Chee, FC, Burke, RD. 2007, Apical organs in echinoderm larvae: insights into larval evolution in the Ambulacraria. *Evol. Dev.*, 9, 432–445.
69. Holland, L.Z. 2015, The origin and evolution of the chordate nervous systems, *Phil. Trans. R. Soc. B*, **370**, 20150048.
70. Mashanov, V.S., Zueva, O.R., Rubilar, T., et al. 2016, Echinodermata. In: Schmidt-Rhaesa A, Harzsch S, Purschke G. eds, *Structure and Evolution of Invertebrate Nervous Systems*, Oxford University Press: Oxford, pp. 665–688.
71. Byrne, M., Mazzone, F., Elphick, M.R., et al. 2019, Expression of the neuropeptide SALMFamide-1 during regeneration of the seastar radial nerve cord following arm autotomy, *Proc. R. Soc. B*, **286**, 20182701.
72. Byrne, M. 2020, The link between autotomy and CNS regeneration: echinoderms as non-model species for regenerative biology, *BioEssays*, **42**, 1900219.
73. Heinzeller, T. and Welsch, U. 2001, The echinoderm nervous system and its phylogenetic interpretation. In: Roth G, Wullimann MF, eds, *Brain Evol. Cognition*, Wiley: NY, pp. 41–47.